Conformational Effects on the Photophysics of Conjugated Polymers: A Two Species Model for MEH−PPV Spectroscopy and Dynamics

Christopher J. Collison,* Lewis J. Rothberg, Varaporn Treemaneekarn, and Yi Li

Department of Chemistry, Hutchison Hall, University of Rochester, Rochester, New York 14627

Received August 1, 2000; Revised Manuscript Received January 17, 2001

ABSTRACT: We report transient and steady state photoluminescence results along with absorption and NMR data to support the existence of two distinct morphological species in MEH−PPV solutions. NMR data provide evidence for the close packing of polymer chains, a consequence of solvent quality reduction. These data are correlated with optical properties of the aggregated species in poor solvents and the isolated chains in good solvents. We infer that steric hindrance of backbone motions increases effective conjugation length and leads to a spectral red shift in absorption and emission. At the same time, interchain excitations with negligible luminescence can be formed, leading to a dramatic reduction in photoluminescence quantum yield. While spectral changes are observed as packing is induced, we show that interchain state formation and its subsequent back-transfer to excitons are particularly sensitive to the interchain registry of the highly packed chains.

Introduction

Conjugated polymers have generated much enthusiasm because of their potential in making organic light-emitting diodes.[1] One polymer of interest is poly-2-methoxy-5-(2′ethylhexoxy)phenylenevinylene, MEH−PPV (Figure 1). Its rigid-rod poly(phenylenevinylene) backbone is combined with alkoxy side groups that provide a solvent skin which contributes the necessary conformational degrees of freedom to ensure solubility and tractability. This facilitates the direct processing of devices. The "hairy rod" style of macromolecule was described well by Wegner in 1993.[2] These side groups usually cause the polymers to assume a glasslike morphology in the solid state, and order on >10 nm length scales is uncommon as measured by transmission electron microscopy or X-ray diffraction.[3] Nevertheless, there is good reason to believe that order is critical in determining the photophysical properties of conjugated polymer films.[4−7] Short-range order appears to be responsible for a significant reduction of luminescence yield in films relative to solution. Formation of nonemissive or weakly emissive interchain excited states is enhanced where chains become efficiently packed.[8] These states act as a sink for potentially useful excitation energy so that a dramatic reduction in quantum efficiency is observed.[9,10] Many chain-separation techniques have been applied to similar polymers in an attempt to reduce the diversion of the emissive excited state to such traps. The success of adding bulky side groups onto the conjugated backbone,[11] deliberate introduction of *cis*-vinylene linkages,[12] and synthesis of block copolymers[13] has been limited. In this work, we investigate the microscopic ordering that leads to reduced photoluminescence (PL) by interpreting optical and magnetic resonance data.

We have chosen to work in solution for four reasons. First, it is easy to controllably realize both the isolated chain, high PL quantum yield geometry as well as the filmlike, aggregated chain, low PL quantum yield configuration. Second, it eliminates the complex and variable spin-casting process used to form films. Third, it facilitates use of NMR techniques, chosen as an independent probe of aggregation and short-range intermolecular order. Finally, the order in films formed by printing or spin-casting is likely to be at least partly related to what is observed in the solutions from which they are formed.[14,15]

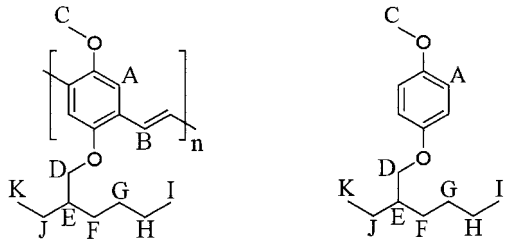

Figure 1. Poly-2-methoxy-5-(2′ethylhexoxy)phenylenevinylene (MEH−PPV), **1**, and 4-(2′-ethylhexoxy)methoxybenzene, **2,** with key to proton assignments in NMR spectra.

Our observations can be summarized as follows: reduction of solvent quality leads to a diminution of the magnetic resonance signature. We argue that this reflects a loss of motional averaging[16] due to steric constraints on the polymer backbone motions that is caused by aggregation of the chains. These phenomena coincide with dramatic changes in optical absorption and emission spectra, excited state decay dynamics, and PL quantum yield as we reduce solvent quality. The structural change and backbone alignment we induce by solvent quality reduction is consistent with work by Huser,[15] Hu,[17] and Nguyen.[18] From these observations, our primary conclusions are the following:

(1) Both absorption and PL spectra can be quantitatively understood in terms of only two types of chain environments. We refer to these as "isolated" and "well-packed".

(2) The chains in well-packed regions are characterized by loss of motional averaging in NMR and red-shifted absorption and emission. In addition, the luminescence quantum yield in these regions is dramatically reduced relative to isolated regions.

(3) Even in well-packed regions, the emission spectrum is best understood as that of a single chain, the

10.1021/ma001354d CCC: $20.00
Published on Web 02/20/2001

Table 1. Assignment of ^{1}H NMR Peaks to Protons of 1, Poly-2-methoxy-5-(2′-ethylhexoxy)phenylene Vinylene (Polymer), and 2, 4-(2′-Ethylhexoxy)methoxybenzene, in Deuterated Toluene; Units Are in ppm Chemical Shift Relative to Tetramethylsilane

proton label	A	B	C	D	E	I, K	G, H	F, J
1 in $C_6D_5CD_3$/ppm	8.02	7.52	3.48	3.40−4.10	1.82	0.94−0.93	1.35	1.50−1.76
2 in $C_6D_5CD_3$/ppm	6.79−7.18		3.369	3.632−3.645	1.626	0.89	1.26	1.40

red shift being caused primarily by increased conjugation length due to suppression of torsional motion. There is no need to invoke ground state dimers/aggregates to understand the spectroscopy of MEH−PPV films.

(4) The reduction in quantum yield in well-packed regions is *not* accompanied by a reduction in excited state lifetime. We attribute the low emission efficiency to rapid formation of nonemissive interchain species in the well-packed regions.

The implications for design and processing of conjugated polymers to make devices will be discussed.

Experimental Section

MEH−PPV was prepared via a modified Gilch route, purified, and characterized as described elsewhere.[19] MEH−PPV obtained from the modified Gilch route typically has very high purity and very low chlorine content. The weight-averaged molecular weights of two MEH−PPV samples synthesized in our group were found to be 7.9 and 1.0 MDa, and their respective polydispersities were 18.4 and 7.6. The second smaller molecular weight sample was used to demonstrate the intrinsic nature of our observations. The resulting solid was kept in the dark when not in use. Stock solutions were made up by adding solid to toluene solvent and sonicating for a time period ranging from hours to days. The resulting solution was filtered through a 0.45 μm filter; we found that solutions made purely by stirring our solid over a period of days were better described as suspensions and would not pass through the same type of filters. Hexane and toluene were added to this stock solution to make up the required concentrations and quality of solvent. Observable changes in color to solutions on reducing solvent quality were instantaneous. We infer that the rate of formation of any packed states is extremely fast. All measurements were carried out on these solutions on the day of their preparation. All solvent mixtures are reported as a volume fraction of toluene vs total volume. All solutions used in optical characterization were clear, and precipitation was not evident to the naked eye.

For optical measurements in different solvent mixtures, many samples with equal polymer concentrations were prepared. Optical densities of the solutions studied were less than 0.1 at absorption maximum in a 1 cm path length cuvette. Low concentrations were used for all optical measurements because of the high sensitivity of UV−vis absorption (vs NMR) and to eliminate the risk of introducing self-absorption artifacts in fluorescence.

For NMR experiments MEH−PPV/toluene stock solutions were diluted by adding hexane or cyclohexane. This allowed use of a single 5 mm tube such that the conditions could be kept constant for the duration of each experiment. After each addition of poor solvent the volume fraction of toluene was calculated, and an NMR spectrum was recorded. Integrals of all peaks, including the toluene 2.09 ppm peak, were calculated with Bruker XWINNMR software. These integrals were calibrated for each spectrum to a value of 1.00 for the toluene protons observed at 2.09 ppm. Calibrated MEH−PPV peak intervals were compared from one solvent mixture to the next. Hexane/toluene data are not tabulated here because quantitative interpretations are limited by the overlap of polymer alkyl peaks with deuterated hexane peaks.

Concentrations used were of the order of 1−2.5 mg/mL. These concentrations were too optically dense for the UV−vis spectrometer despite using a 1 mm cuvette. The same spectral shifts due to solvent quality do occur with high concentrations of MEH−PPV where the limit of the UV−vis spectrometer is approached. It is likely therefore that any changes in NMR spectra with solvent correspond to changes in absorption and fluorescence with solvent especially in light of the high rate of formation of packed samples in the dilute case. NMR collection parameters were kept constant throughout these experiments. Thorough shimming was carried out such that peak integration would be as accurate as possible. All solvents used for NMR characterization were deuterated (chloroform-d_1 DLM-7, toluene-d_8 DLM-5, *n*-hexane-d_{14} DLM-139, and cyclohexane-d_{12} DLM-17; Cambridge Isotope Laboratories, Inc.). NMR spectra were recorded on a Bruker AMX 400 MHz.

Luminescence spectra were recorded on a SPEX photon-counting Fluorolog-2 spectrofluorimeter using DM3000F software, with an in-built reference quantum counter to correct for excitation intensity fluctuations. The spectra were corrected for the wavelength response of the detection system. Quantum efficiencies of the same sample in different solvent mixtures were measured relative to Rhodamine 6G in dilute ethanol solution according to Rhys Williams et al.[20] The solutions studied in the spectrofluorimeter were dilute (absorbance maximum <0.1) and were measured separately in a right angle instrument geometry and a front face instrument geometry to rule out inner filter effects. We have found the spectral changes to be intrinsic for MEH−PPV and largely independent of average molecular weight.

Luminescence decays were measured using time-correlated single-photon counting.[21] The sample was excited by the output of a cavity-dumped dye laser which was synchronously pumped by a frequency-doubled mode-locked Nd:YLF laser. The dye laser generated light pulses of 10−15 ps duration at a 1.9 MHz repetition rate. The excitation wavelength was either 575 or 568 nm at <0.5 nJ/cm^2 fluences (<1 mW/cm^2), and a microchannel plate photomultiplier tube (Hamamatsu R1564U-07) was used to detect the fluorescence after its pass through a monochromator. The apparatus produces an instrument response function of fwhm less than 80 ps. Luminescence decays were analyzed in terms of the sum of exponentials using a nonlinear least-squares iterative reconvolution procedure.[21]

Results and Discussion

We illustrate the aggregation phenomenon in MEH−PPV by presenting results from NMR spectra recorded after addition of poor solvent to stock MEH−PPV solutions in toluene. The ^{1}H NMR assignments of MEH−PPV in toluene are shown in Table 1 corresponding to the labeling in Figure 1. These assignments are shown alongside those for 4-(2′-ethylhexoxy)methoxybenzene[22] in toluene for comparison.

Integrated intensities for NMR peaks of MEH−PPV in volume fractions of toluene and cyclohexane are shown in Table 2. In several repetitions of this experiment with different solutions prepared in slightly different ways the results are the same. The concentration of toluene in each solvent mixture decreases at exactly the same rate as the concentration of polymer. Yet there is a decrease in MEH−PPV integrated intensity relative to toluene through successive solvent mixtures, shown clearly for all MEH−PPV protons presented in Table 2a. This gives a clear indication of the degree of polymer aggregation with addition of poor solvent. Upon aggregation configuration averaging is reduced, and a given proton under study fails to sample many of its possible positions on the time scale of the nuclear spin relaxation. In this way, dipole−dipole coupling is the

Table 2. Selected NMR Integrated Intensities of (a) 7.8 MDa and (b) 1.0 MDa MEH−PPV[a]

% toluene	phenyl protons A (÷2)	OCH protons C, D (÷5)	methyl protons I, K (÷6)	toluene protons
		(a) 7.8 MDa		
100	0.128 ± 0.001 (0.064)	0.621 ± 0.024 (0.124)	1.092 ± 0.014 (0.182)	1
80	0.090 ± 0.004 (0.045)	0.452 ± 0.001 (0.090)	0.829 ± 0.012 (0.138)	1
70	0.081 ± 0.001 (0.041)	0.416 ± 0.017 (0.083)	0.755 ± 0.004 (0.126)	1
60	0.063 ± 0.011 (0.031)	0.332 ± 0.028 (0.066)	0.590 ± 0.048 (0.098)	1
50	0.011 ± 0.001 (0.005)	0.109 ± 0.002 (0.022)	0.306 ± 0.117 (0.051)	1
40	0.003 ± 0.001 (0.002)	0.060 ± 0.001 (0.012)	0.262 ± 0.105 (0.044)	1
		(b) 1.0 MDa		
100	0.133 ± 0.001 (0.067)	0.500 ± 0.008 (0.100)	0.680 ± 0.001 (0.113)	1
80	0.124 ± 0.001 (0.062)	0.473 ± 0.001 (0.096)	0.662 ± 0.003 (0.110)	1
60	0.082 ± 0.001 (0.041)	0.351 ± 0.001 (0.070)	0.516 ± 0.001 (0.086)	1
50	0.058 ± 0.002 (0.029)	0.235 ± 0.007 (0.047)	0.409 ± 0.002 (0.068)	1
40	0.038 ± 0.004 (0.019)	0.169 ± 0.006 (0.034)	0.308 ± 0.004 (0.051)	1
30	0.040 ± 0.004 (0.020)	0.175 ± 0.007 (0.035)	0.280 ± 0.010 (0.047)	1
20	0.036 ± 0.004 (0.018)	0.173 ± 0.018 (0.035)	0.300 ± 0.029 (0.050)	1

[a] Normalized to integrated intensity of toluene 2.09 ppm multiplet for each toluene:cyclohexane solvent mixture. Values in parentheses are scaled to represent integrated intensity per proton.

mechanism leading to inhomogeneous broadening, in some cases to an extent that peaks become indistinguishable from the baseline.

It is also apparent that the signal strength of the phenyl protons, A, is decreasing relative to that of the terminal alkyl methyl protons, I and K. We believe this to be indicative of further reduction of configuration averaging in the backbone protons relative to the alkyl chain protons, perhaps caused by torsional restraint, absent in the side groups, imposed by chain packing.

We repeated our NMR experiment on an MEH−PPV polymer of significantly lower molecular weight. These results are shown in Table 2b. While the general trends are the same and aggregation is shown by a drop in integrated intensity relative to toluene, the difference between backbone and alkyl protons is much less significant. We believe this may be as a result of the different propensities for the chain to fold back upon itself for different molecular weights. We defer discussion of the exact mechanism for aggregation to subsequent work.

In summary, by adding hexane or cyclohexane to toluene solutions, the solubility (Hildebrandt) parameter[23] of the solvent is changed and the polymer responds by becoming less solvated. The protons are severely restricted in a nonsolvated packed geometry. The MEH−PPV peaks become indistinguishable from the background, and the toluene peaks do not. Independent of how well the NMR data describe it, a likely result of MEH−PPV packing is the damping of ring torsion due to steric hindrance from adjacent chains.

Absorption and emission spectra of MEH−PPV in toluene and hexane mixtures are shown in Figure 2. As hexane proportion is increased, absorption intensity is reduced (Figure 2a), a red shift is apparent, and structure is seen to develop. In Figure 2b, the dramatic effect of decreasing solvent quality on fluorescence is shown. There is an overall red shift in the peak of the emission, and the quantum yield drops by about 3 times as the fraction of toluene drops to 10%.

It is worth considering whether the effect of changing dielectric properties of the solvent can be responsible for the changes in the photophysics. The decreased orientation polarizability[24] of hexane should lead to a blue shift, by relative destabilization of the larger dipole moment of the excited state, and is therefore *not* possible as an explanation for this overall red shift. We have found empirically that spectroscopic changes like those of Figure 2 are uncorrelated with dielectric properties of solvents and are very sensitive to the solvent quality.

The effects of solvent quality on the fluorescence are inconsistent with a change in the Franck−Condon envelope for the transition. The Franck−Condon envelopes of the 0% hexane and 90% hexane samples are nearly identical (Figure 2c) even though the mixtures in between appear very different. We therefore expect the equilibrium geometries of the two species with these spectra to be similar and think it is most reasonable to consider them both intrachain excitations. We hypothesize that these spectra reflect two types of chain with different conjugation lengths. With decreasing quality of solvent the chains start to aggregate in order to minimize interactions with the poor solvent. It is likely that torsional motion along the backbone is suppressed by the presence of adjacent chains. In turn, removal of low-energy rotations and vibrations along the backbone of a conjugated polymer chain increases conjugation length.[25] We believe that this explains the red-shifted spectrum with similar Franck−Condon envelope. The increased order and suppression of ring torsion are also reflected in the increase in structure observed in the absorption of the 10% toluene samples (Figure 2a).

Given our picture, we should be able to decompose the absorption and emission data into a sum of absorption and emission spectra of the two extremes. Absorption provides us with a more accurate representation of the amounts of the two types of chain since the technique is indiscriminate. PL may be more complicated in terms of the fractions of each type of chain present since we will observe luminescence from low-energy regions preferentially, as a result of energy transfer.[26,27] For the same reason, however, it is easier in PL to realize the extreme cases experimentally since any excitation onto isolated chains in a cluster containing well-packed chains will result in packed chain emission.

Figure 3 illustrates that we can indeed reconstruct the fluorescence spectrum of the 60% toluene: 40% hexane solution from a linear combination of our 100% and 10% cases. The results provide qualitative support for the two species model and provide a description of the interplay between the two configurations.

Analogous reconstruction of absorption spectra can be demonstrated. However, we would be able to do this even if these cases were not extremes. Therefore, we show, in Figure 4, what happens if we assume that in 100% toluene we have only isolated chains, but in our

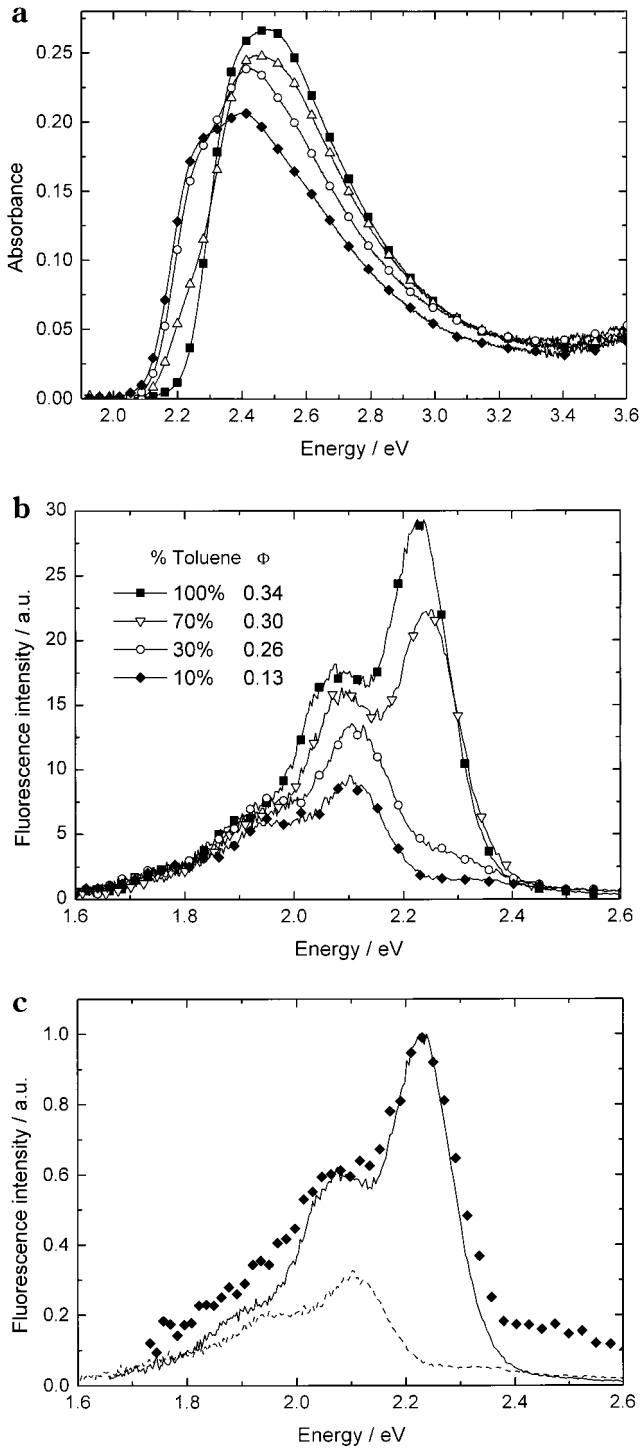

Figure 2. Absorption and fluorescence emission data of MEH−PPV polymer in various toluene:hexane solvent mixtures. For absorption spectra (a), square represents 100:0; triangle, 50:50; circle, 30:70; and diamond, 10:90. For emission spectra (b) excited at 420 nm (2.96 eV), square represents 100:0; triangle, 70:30; circle, 30:70; and diamond, 10:90. Quantum efficiencies are shown in the accompanying legend. (c) shows emission spectra (2.96 eV excitation) of the two measured extremes, 100% toluene (solid) and 10% toluene: 90% hexane (dash). Diamonds represent an adjusted 10:90 solvent mixture blue-shifted and enlarged for comparison with the 100% toluene emission spectrum.

worst case (10% toluene) we still have isolated chains among the well-packed regions. We can then subtract the spectrum for the isolated chains from our worst case to simulate this. With this procedure, the absorption of our extrapolated worst case spectrum can be made to look like a mirror image of the PL, in contrast to what is seen in most phenylenevinylene polymers. We believe the effect of side-chain steric hindrance is a locking of the backbone and reduction of torsional motions about the axis defined by the chain. This is consistent with singlet−singlet $S_0 \rightarrow S_1$ absorption on locked chains being a mirror image of fluorescence spectra since little reorganization can occur. The worst case spectrum is also relatively well resolved since the many low-frequency backbone torsions, which would otherwise broaden and obscure the spectrum, are frozen out by the restrictive geometry of the polymer in these clusters. The importance of torsion in the spectroscopy is apparent in the lack of structure in PPV oligomer absorption, which occurs despite the uniformity of conjugation length. When the molecules are not heavily constrained, the initial excitation energy will couple to the backbone torsions in isolated MEH−PPV in the same way that *trans*-stilbene twists upon photoexcitation.

A summary of the results from our decompositions is given in Figure 5. We compare absorption and PL coefficients, defined below, and the NMR integrated

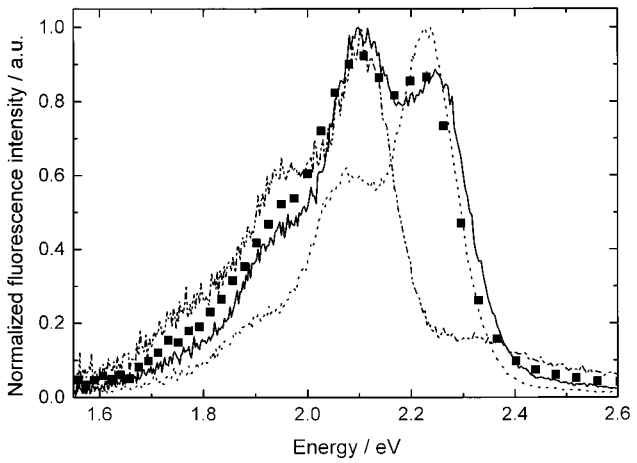

Figure 3. Reconstruction (solid squares) of the measured 60:40 toluene:hexane fluorescence emission spectrum (solid line) from linear combination of 100:0 emission (dotted line) and 10:90 emission (dot−dot−dash).

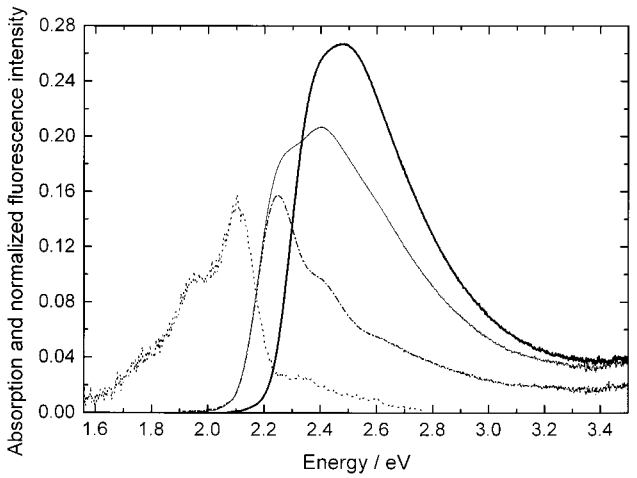

Figure 4. Absorption spectra of 100% toluene solution (heavy solid), 10:90 toluene:hexane solution (solid) together with an absorption spectrum of the extreme well-packed state (dot−dash) inferred by subtraction of good solvent absorption from poor solvent absorption. Fluorescence emission spectrum (2.96 eV excitation) of 10:90 solution is shown (dot−dot) for mirror-image comparison.

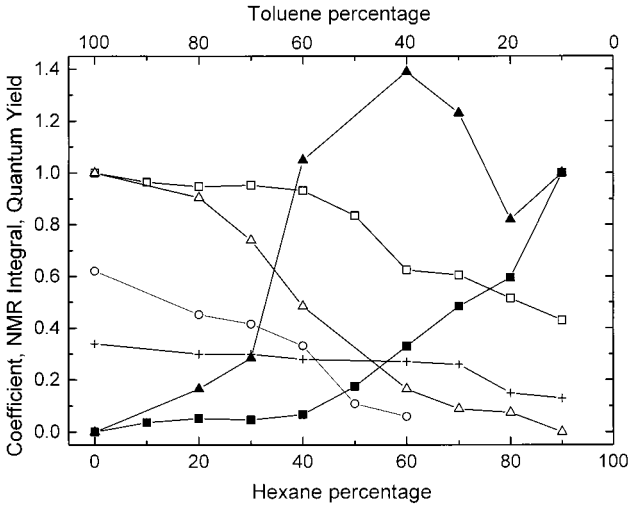

Figure 5. Compilation of absorption (squares) and emission (triangles) coefficients, and NMR integrated intensity (O−C−H protons) normalized to toluene 2.09 ppm multiplet (circles). "Good" (open symbols) and "bad" (solid symbols) coefficients are generated in eq 1 and plotted. PL quantum yield of dilute solution is shown (plus signs).

intensities for the five OCH protons arbitrarily normalized to the toluene peak (from Table 2a) in each case. The fits for absorption (Absn) and fluorescence (PL) respectively are

$$\mathrm{Fit_A} = g_\mathrm{A}\mathrm{Absn}_{100\%\mathrm{toluene}} + b_\mathrm{A}[\mathrm{Absn}_{10\%\mathrm{toluene}} - 0.43\mathrm{Absn}_{100\%\mathrm{toluene}}]$$

$$\mathrm{Fit_{PL}} = g_\mathrm{PL}\mathrm{PL}_{100\%\mathrm{toluene}} + b_\mathrm{PL}\mathrm{PL}_{10\%\mathrm{toluene}}$$

where g is the coefficient dictating the contribution from the good solvent spectrum and b is the coefficient for the bad solvent, well-packed sample contribution. We normalize to $\mathrm{Absn}_{100\%\mathrm{toluene}}$ for the absorption fits since the absorption due to aggregated species will continue to decrease with decreasing solvent quality. Aggregate absorption decreases as a result of the drop in effective aggregate concentration, caused by aggregate size increases and a fixed number of polymer chains in the system under study.

In Figure 5, we further note the correlation of the absorption "good" coefficient with the NMR intensity. This is consistent with the fact that both techniques are sensitive to the actual amounts of isolated chain species present in the sample.

Of particular interest is the trend in PL coefficients. The "good" PL coefficient starts to significantly drop between 20 and 30% hexane whereas the onset for significant change in absorption occurs between 40 and 50%. This is explained by considering that upon physical aggregation many chains within a cluster will be exposed. These exposed sections will act as isolated chains but, since tethered to a packed unit, will allow energy transfer to the well-packed regions where emission occurs.[15,18] Another interesting observation from the fits is that we need coefficients greater than unity to fit the spectra of solutions in the 40−75% hexane range; i.e., we need more "bad" PL at 70% than at 90% hexane to fit the data. This is true even though the PL over the range from 70 to 90% is essentially all from packed regions. It follows that the average cluster size increases and/or that the chains become more ordered having the effect of increasing the number of potential

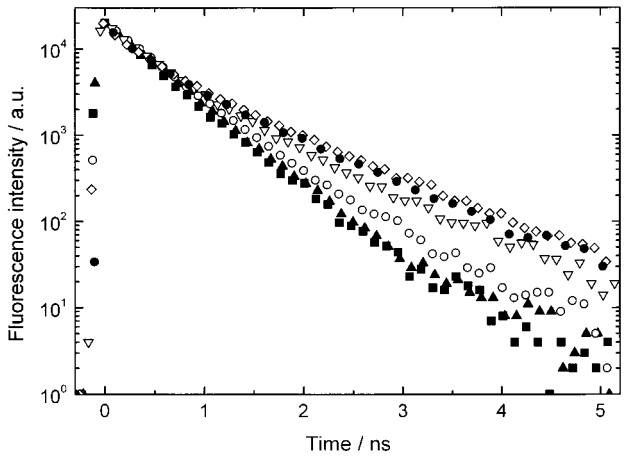

Figure 6. Fluorescence decays of MEH−PPV in toluene: hexane solvent systems; 100:0, solid square; 70:30, solid triangle; 50:50, open circle; 30:70, open triangle; 10:90, open diamond; thin film, solid circle. All decays were measured at an emission wavelength of 640 nm (1.94 eV). Solutions were photoexcited at 568 nm (2.19 eV) and the film was excited with 575 nm (2.16 eV) light.

sites where nonemissive interchain species can form. This explains the continued reduction in PL yield and is consistent with the large body of work on anomalous long-lived decay dynamics in PPV.[10,28]

We sum up with the following three cases. In 100% toluene we see fluorescence from isolated chains with a quantum efficiency of 34%. In the range 30−60% toluene, there is a decreasing amount of fluorescence from isolated chains because of energy transfer to longer conjugation lengths, only some of which may be well enough packed to participate in interchain state formation. There will also be a small amount of fluorescence as a result of direct excitation of longer conjugation lengths as evidenced by an increase in "poor" absorption coefficient. In the 10% toluene solution, interchain excited state formation dominates the relaxation pathways open to the initially photogenerated states. There will be substantially more direct excitation of long conjugation length species, but even with the possibility of back-transfer[28,29] from interchain excited states to singlets, the fluorescence is lowest in this solution. We believe this confirms the mechanism for reduction of fluorescence in the solid state as being interchain excited state formation.

The fluorescence decays for MEH−PPV solutions, of equal concentration but varying solvent quality, are shown in Figure 6. These solutions are excited at 568 nm and are compared with a film excited at 575 nm. The decays of good solvent solutions are almost monoexponential. As solvent quality is reduced, the overall decay time *increases* (even though the PL yield *decreases*), but significantly, most of the change occurs after 500 ps. The decay for 90% hexane/10% toluene is almost identical to the decay of a thin film of the same sample. This suggests that the well-packed MEH−PPV in solution is a reasonable proxy for thin films of MEH−PPV.

We ascribe the rapid decay component (∼0.3 ns) to directly excited singlet state emission, an extrapolation from the 100% toluene case. The long-lived fluorescence decay is associated with the singlet state following back-transfer from nonemissive interchain excited states to intrachain excited states. This latter assignment is corroborated by the observation that there is very little

Table 3. Fitting Parameters for Sum of Three Exponentials Description of Fluorescence Decay Excited at 568 nm and Detected at 640 nm (a) and 780 nm (b)[a]

% toluene	Tau 1/ps ± 10 ps	% of total PL	Tau 2/ps ± 10%	% of total PL	Tau 3/ps ± 10%	% of total PL	Φ ± 10%
			(a) Detected at 640 nm				
100	30	5	240	30	495	65	0.34
80	90	5	360	60	600	34	0.30
60	170	7	400	72	650	21	0.28
50	130	4	390	66	700	30	
40	80	6	405	63	810	31	0.27
30	60	7	360	45	820	48	0.26
20	50	7	310	31	840	61	0.15
10	60	7	320	29	945	64	0.13
			(b) Detected at 780 nm				
100	70	6	390	70	680	25	0.34
80	110	6	440	85	1110	9	0.30
70	80	3	430	87	1030	9	0.30
60	170	5	450	88	1290	7	0.28
50	190	6	480	81	1230	13	
40	60	4	450	66	1010	30	0.27
30	60	5	440	50	970	46	0.26
20	40	3	420	31	950	65	0.15
10	80	3	520	35	1080	62	0.13

[a] Decay times, Tau *n*, are given in picoseconds. For each decay time, the contribution to the decay is presented as a percentage of the full integrated intensity $a_1\tau_1/(a_1\tau_1 + a_2\tau_2 + a_3\tau_3) \times 100\%$, where a_n is the preexponential factor and τ_n is the decay time. The luminescence efficiency, Φ, for the solutions is presented for comparison.

change to the emission spectrum with time in the long-lived tail.

The decays can be parametrized well by three exponentials, giving fits of χ^2 less than 1.3. This parametrization is a descriptive tool, and the long components of the decay can be correlated with the gradually increasing solid state character of the samples. We use three exponentials as a matter of convenience without intending specific physical meaning for these decay times. Attributing exponentials to fluorescence from excited states that have evolved (from the initially photogenerated state) by hopping and/or back-transfer from interchain states is not expected to be valid since back-transfer from polaron pairs is likely to occur with a distribution of rates.[28]

In a given solution, depending on the relative absorption of each species at that wavelength, we can excite both isolated segments and well-packed segments directly. Isolated segments will likely transfer their energy to nearby well-packed segments that can emit, or to "well-packed-registered" segments, defined by their ability to form interchain nonemissive states or polaron pairs. Directly excited well-packed segments may also transfer their energy to well-packed-registered sequences to form the nonemissive states.

Analysis of Table 3 provides strong evidence for these two types of locations within packed areas. The presence of long decay times (>600 ps at 640 nm and >1000 ps at 780 nm), assigned to back-transfer, in solutions of 80% toluene and below, reflects the existence of well-packed-registered chains. The onset of their existence coincides exactly with the drop in good fluorescence coefficient, g_{PL}, observed in Figure 5 at 80% toluene. Furthermore, the drop in PL efficiency between 30 and 20% toluene correlates well with sudden changes in the dominant decay component (Tau 3; 48−61% and 46−65% at 640 and 780 nm, respectively).

In the 10% toluene case, with 568 nm (2.19 eV) excitation, over 96% of the absorbing species are well-packed species. From our temporal fits, 64% of the integrated emission is associated with the long decay and back-transfer. Less than 30% of the emission is assigned to PL from the directly excited singlet. This correlates with the drop of quantum efficiency of just over a third, from 0.34 to 0.13 in our solutions and the 0.35 to 0.10 drop from solution to film given in the literature.[9,30]

The quantum yield of photoluminescence can be described as follows for direct excitation of well-packed sequences,

$$\Phi_{PL} = (1 - \Phi_{P^+-P^-})\Phi_{S_1} + \Phi_{P^+-P^-}\Phi_{BT}\Phi_{S_1}$$

where $\Phi_{P^+-P^-}$ is the quantum yield of interchain excited state formation, Φ_{S_1} is the luminescence quantum yield of singlet excitons, and Φ_{BT} is the quantum efficiency for back-transfer from the interchain state to the singlet state. We then substitute values derived from our worst case emission spectrum (0.13 and 0.34) for Φ_{PL} and Φ_{S_1}, respectively. The integrated intensity percentage of long decay fluorescence, 64% (Table 3), assumed to be representative of back-transfer, is used as a multiplier to adjust the Φ_{PL} of 0.13 and equate it to the whole term $\Phi_{P^+-P^-}\Phi_{BT}\Phi_{S_1}$. From this, we obtain a value for $\Phi_{P^+-P^-}$ of 0.86 and, in turn, a value for Φ_{BT} of 0.28. This value for the quantum yield of back transfer may be significant in that it is essentially $^1/_4$. The model of Dyakonov et al.[31] suggests that when interchain states are formed, there is some degree of charge separation such that opposite charges reside on the two chains sharing the excitation. At room temperature these interchain states do not emit, and possible relaxation pathways are spin-dependent geminate recombination to form the intrachain state or dissociation into free charge carriers. From our calculation it appears that, in the absence of an applied field, recombination is certain but in the 1:3 ratio of singlets to triplets. This may support the simple spin-statistical result determining the 25% theoretical upper limit of EL yield for polymer LEDs.

This calculation is simplified in the worst solvent case since, with 568 nm excitation, over 96% of the absorbing species are well-packed sequences. Since rates and efficiencies of energy transfer will be different from isolated sequences to well-packed sequences, we cannot easily apply this approach to solutions with better solvent quality.

Conclusion

We provide transient and steady state fluorescence results, absorption and NMR data to support the existence of two distinct morphological species in MEH−PPV. To a good approximation, the large inhomogeneities in local environment are overwhelmed by a single feature of the morphology that dominates the photophysics. The implications for understanding the spectroscopy and PL quantum efficiency of conjugated polymers in general are far-reaching. Furthermore, simple spectral analyses of films made under different processing conditions may be instructive in predicting device efficiency.

In good solvents there exist isolated segments with short conjugation lengths primarily delimited dynamically by thermally excited ring torsion along the chain backbones. In poor solvents well-packed chains, which in our opinion are torsionally restricted, are formed to avoid polymer−solvent interactions. Solvent-induced packing leads to chains best described as locally ordered. These seem to be an excellent model for the microscopic description of the polymer in thin films as are used in organic LEDs. The effect of these domains can be seen in low-concentration solutions so that quantum efficiencies can be measured with respect to a standard.[20] The large number of sites sampled in any given experiment, because of the ability of the chromophores to move around, avoids sample degradation caused by repetitive excitation of small numbers of sites in thin films.

We show that the well-packed regions in MEH−PPV probably have absorption spectra that are a mirror image of their fluorescence spectra. This is *not* the case in the isolated chain case where the spectrum is much broader and less well resolved than the corresponding fluorescence. These properties have been previously attributed to a spread of absorbing conjugation lengths. We think it is more likely that the breadth and low resolution of the absorption spectrum have come about as a result of numerous rovibronic states of the less rigid isolated backbone that are very close in energy in isolated chains but are frozen out by chain packing.

We have shown that the degree of packing, on a microscopic level, reduces the quantum efficiency by as much as $^2/_3$. The measured drop in quantum efficiency correlates to changes in steady state spectroscopy and a long-lived tail to the PL. There is *not*, however, a significant change in singlet lifetime. Since there are no spectral dynamics, our data provide evidence for the long tail in the PL decay of MEH−PPV being a result of back transfer from a nonemissive interchain excited state to the intrachain singlet. While energy transfer to longer conjugation lengths is enhanced as packing is *induced*, it appears that interchain state formation and subsequent back-transfer are highly sensitive to the interchain registry of the packed chains. This pathway for excitation energy dominates in only the samples with very low solvent quality that resemble the fully aggregated case of solid thin films. Our data are consistent with a quantum yield for back transfer to the singlet close to $^1/_4$, which lends some support to the idea that reduction of PL in the aggregated case is due to triplet formation upon recombination of polaron pairs. This implies charge separation upon interchain state formation, and further studies are taking place to quantify branching ratios and their variation as a function of morphology.

Acknowledgment. We gratefully acknowledge support from the NSF in Grant CHE 9120001. We also thank Sandip Sur for valuable help and discussion regarding NMR measurements.

References and Notes

(1) Burroughes, J. H.; Bradley, D. D. C.; Brown, A. R.; Marks, R. N.; Mackay, K.; Friend, R. H.; Burns, P. L.; Holmes, A. B. *Nature* **1990**, *347*, 539−541.
(2) Wegner, G. *Mol. Cryst. Liq. Cryst.* **1993**, *235*, 1−34.
(3) Masse, M. A.; Martin, D. C.; Thomas, E. L.; Karasz, F. E.; Petermann, J. H. *J. Mater. Sci.* **1990**, *25*, 311−320.
(4) Chen, S. A.; Chang, E. C. *Macromolecules* **1998**, *31*, 4899−4907.
(5) Strehmel, B.; Sarker, A. M.; Malpert, J. H.; Strehmel, V.; Seifert, H.; Neckers, D. C. *J. Am. Chem. Soc.* **1999**, *121*, 1226−1236.
(6) Hide, F.; DiazGarcia, M. A.; Schwartz, B. J.; Andersson, M. R.; Pei, Q. B.; Heeger, A. J. *Science* **1996**, *273*, 1833−1836.
(7) Grell, M.; Bradley, D. D. C.; Long, X.; Chamberlain, T.; Inbasekaran, M.; Woo, E. P.; Soliman, M. *Acta Polym.* **1998**, *49*, 439−444.
(8) Jakubiak, R.; Collison, C. J.; Wan, W. C.; Rothberg, L. J.; Hsieh, B. R. *J. Phys. Chem. A* **1999**, *103*, 2394−2398.
(9) Samuel, I. D. W.; Rumbles, G.; Collison, C. J. *Phys. Rev. B: Condens. Matter* **1995**, *52*, 11573−11576.
(10) Yan, M.; Rothberg, L. J.; Kwock, E. W.; Miller, T. M. *Phys. Rev. Lett.* **1995**, *75*, 1992−1995.
(11) Bao, Z. N.; Amundson, K. R.; Lovinger, A. J. *Macromolecules* **1998**, *31*, 8647−8649.
(12) Son, S.; Dodabalapur, A.; Lovinger, A. J.; Galvin, M. E. *Science* **1995**, *269*, 376−378.
(13) Hu, B.; Karasz, F. E. *Synth. Met.* **1998**, *92*, 157−160.
(14) DiazGarcia, M. A.; Hide, F.; Schwartz, B. J.; McGehee, M. D.; Andersson, M. R.; Heeger, A. J. *Appl. Phys. Lett.* **1997**, *70*, 3191−3193.
(15) Huser, T.; Yan, M.; Rothberg, L. J. *PNAS* **2000**, *97*, 11187−11191.
(16) *A Complete Introduction to Modern NMR Spectroscopy*, 1st ed.; Macomber, R. S., Ed.; John Wiley & Sons: New York, 1997, and references therein.
(17) Hu, D. H.; Yu, Y.; Wong, K.; Bagchi, B.; Rossky, P. J.; Barbara, P. F. *Nature* **2000**, *405*, 1030−1033.
(18) Nguyen, T. Q.; Doan, V.; Schwartz, B. J. *J. Chem. Phys.* **1999**, *110*, 4068−4078.
(19) Hsieh, B. R.; Yu, Y.; VanLaeken, A. C.; Lee, H. *Macromolecules* **1997**, *30*, 8094−8095.
(20) Rhys Williams, A. T.; Winfield, S. A.; Miller, J. N. *Analyst* **1983**, *108*, 1067−1071.
(21) *Time-Correlated Single Photon Counting*; O'Connor, D. V., Phillips, D., Eds.; Academic Press: London, 1984.
(22) Stalmach, U.; Kolshorn, H.; Brehm, I.; Meier, H. *Liebigs Ann.* **1996**, *9*, 1449−1456.
(23) *The Chemistry of Polymers*, 2nd ed.; Nicholson, J. W., Ed.; RSC Paperbacks, Springer-Verlag: Berlin, 1997.
(24) *Principles of Fluorescence Spectroscopy*, 1st ed.; Lakowicz, J. R., Ed.; Plenum Press: New York, 1983.
(25) Pasco, S. T.; Baker, G. L. *Synth. Met.* **1997**, *84*, 275−276.
(26) Heun, S.; Mahrt R. F.; Greiner, A.; Lemmer, U.; Bässler, H.; Halliday, D. A.; Bradley, D. D. C.; Burn, P. L.; Holmes, A. B. *J. Phys.: Condens. Matter* **1993**, *5*, 247−260.
(27) Förster, T. Z. *Ann. Phys. (Leipzig)* **1948**, *55*, 6.
(28) Rothberg, L. J.; Yan, M.; Papadimitrakopoulos, F.; Galvin, M. E.; Kwock, E. W.; Miller, T. M. *Synth. Met.* **1996**, *80*, 41−58.
(29) Rumbles, G.; Samuel, I. D. W.; Collison, C. J.; Miller, P. F.; Moratti, S. C.; Holmes, A. B. *Synth. Met.* **1999**, *101*, 158−161.
(30) Greenham, N. C.; Samuel, I. D. W.; Hayes, G. R.; Phillips R. T.; Kessener, Y. A. R. R.; Moratti, S. C.; Holmes, A. B.; Friend, R. H. *Chem. Phys. Lett.* **1995**, *241*, 89−96.
(31) Dyakonov, V.; Rösler, G.; Schwoerer, M.; Frankevich, E. L. *Phys. Rev. B: Condens. Matter* **1997**, *56*, 3852−3862.

MA001354D